Advances in Nano Research, *Vol. 17, No.3 (2024) 221-234*
https://doi.org/10.12989/anr.2024.17.3.221

Dynamic analysis of nanostructure in improving sports equipment assuming sinusoidal shear deformation theory and numerical solution

Xinrui Yang[1] and Amir Behshad*[2]

[1]*College of Physical Education and Health, East China Normal University, 200241, Shanghai, China*
[2]*Faculty of Technology and Mining, Yasouj University, Choram 75761-59836, Iran*

(*Received April 17, 2024, Revised August 14, 2024, Accepted August 17, 2024*)

Abstract. In this paper, dynamic response of annular nanoplates in improving sports equipment with surface effect embedded by visco Pasternak fractional foundation is studied. Size effects are evaluated by modified couple stress theory (MCST) and the surface effects are considered by the Gurtin-Murdoch theory. The structural damping effect is considered in this research using Kelvin-Voigt model. Sinusoidal shear deformation theory (SSDT) is applied for mathematical modelling of the nanostructure system. The numerical procedure of differential quadrature (DQ) is presented to determine the dynamic deflection as well as dynamic response of the annular nanoplates. The numerical results dynamic deflection of the nanostructure is considering, including material length scale parameter, spring and damper constants of visco-pasternak fractional foundation, geometrical parameters of annular nanoplates, surface stress effects.

Keywords: annular/circular nanoplates; couple stress theories; dynamic response; improving sports equipment; sinusoidal; surface effects

1. Introduction

For the non-polynomial and polynomial shear deformation theories for modelling of structures, there are many work in the literature (Li *et al*. 2023, Wang *et al*. 2023, Sun *et al*. 2024). A multilayered/sandwich triangular finite element applied for the linear and non-linear analyses was studied by Polit and Touratier (2002) based on higher-order shear deformation theory. Dau *et al*. (2004) applied finite element triangular method to analyze the multilayered shells base on non-polynomial higher order theory. Using trigonometric shear deformation theory, Dau *et al*. (2006) investigated nonlinear response of structures with different layers. Ganapathi *et al*. (2004) studied bending/torsional behavior of rectangular piezoelectric laminated composite beams using higher order theory. Blanc and Touratier (2007) studied temperature analysis in laminated thin composites using third order polynomial or trigonometric theory. Dynamic and static response of composite laminated and sandwich shells and plates based on a new higher-order shear deformation theory were studied by Mantari *et al*. (2011). A new shear deformation theory was developed by Mantari *et al*. (2012) for composite and sandwich plates. On the basis of sinusoidal higher order shear deformation theory, Mantari and Granados (2014) presented analysis of functionally graded shells and plates. Mantari and Granados (2015) studied the vibrational analysis of composite advanced plates based on novel shear deformation theory. An analytical solution for the static thermoelastic analysis of laminated simply supported composite plates was presented by Ramos *et al*. (2016) based on Carrera shear deformation theory. Mantari *et al*. (2016) presented various higher order theories for trigonometric and hybrid thermoelastic in laminated sandwich and composite plates. Magneto-thermoelastic response in an infinite medium with a spherical hole in the context of high order time-derivatives and triple-phase-lag model was considered by Allehaibi and Zenkour (2022). Garg *et al*. (2020) studied the vibration, buckling and static response of nano functionally graded sandwich nanocomposite plates/beams/ shells using different higher order theories. Laureano *et al*. (2024a, b) presented exact solutions for cylindrical and spherical panels with clamped boundary supports via a unified Carrera theory. Yarasca *et al*. (2024) investigated optimization of functionally graded plates using parametric higher-order deformation theory. Pham *et al*. (2024) introduced the Monte Carlo simulation and finite element method on the basis of refined first-order shear deformation theory to study the random vibration analysis of functionally graded sandwich plates. The dynamic analysis of a smart rectangular beam in a viscoelastic variable foundation was presented by Shahrany and Zenkour (2024) applying a higher-order shear deformation theory. The formulation of the nth-order shear deformation theory was modified by Bouazza and Zenkour (2024) to discuss the hygrothermal free vibration response of composite laminated plates.

For the field of dynamic and static analysis of structures (Li *et al*. 2024, Sun *et al*. 2023), buckling of sandwich plates with FG-CNT-reinforced layers resting on orthotropic elastic medium using Reddy plate theory was considered by Farrokhian (2022, 2023). Sobhani Aragh (2017). Studied stability analysis of the continuously graded CNT-Reinforced Composite (CNTRC) panel stiffened by rings and stringers.

*Corresponding author, Ph.D.,
E-mail: a.behshad@yu.ac.ir

ISSN: 2287-237X (Print), 2287-2388 (Online)

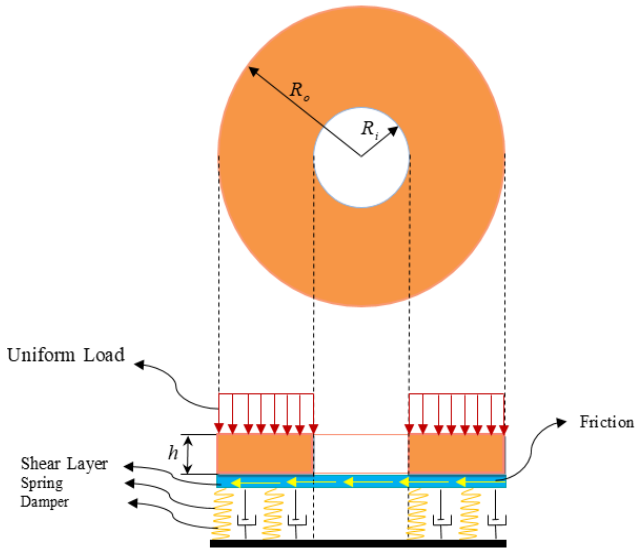

Fig. 1 A schematic of annular nanoplate resting on the frictional viscoelastic foundation

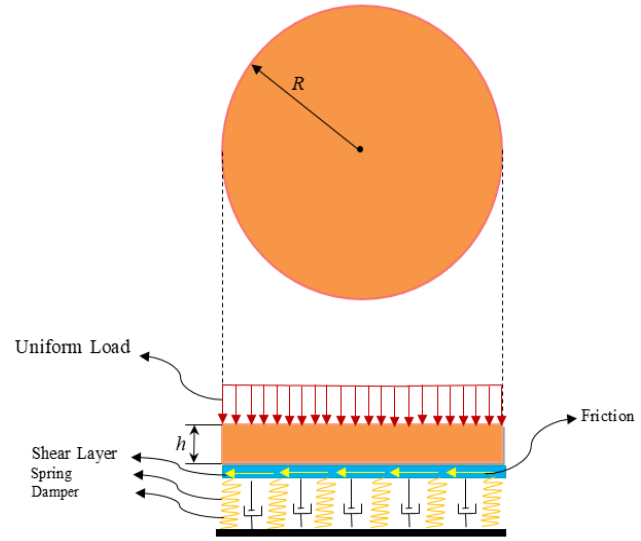

Fig. 2 A schematic of circular nanoplate resting on the frictional viscoelastic foundation

The effect of matrix cracks on the buckling of a hybrid laminated plate as was investigated by Lei and Zhang (2018). Buckling resistance of composite riser always demonstrates diverse sensitivity to the fiber, matrix, and defects were considered by Kang *et al.* (2022). Daikh *et al.* (2020a, b) presented a comprehensive static analysis of simply supported cross-ply carbon nanotubes reinforced composite (CNTRC) laminated nanobeams under various loading profiles. The wave propagation technique was developed by Bahrami and Teimourian (2017) for analyzing the wave power reflection in circular annular nanoplates. The buckling analysis of a cantilever single-walled carbon nanotube embedded in an elastic medium with an attached spring was researched by Yayli (2017). The vibration, buckling and bending analyses of annular nanoplate integrated with piezoelectric layers at the top and bottom surfaces were investigated by Motezaker *et al.* (2017a, b, 2021a, b). Merzouki *et al.* (2021) studied the static response of porous functionally graded nanocomposite beams, with a uniform or non-uniform layer-wise distribution of the internal pores and graphene platelets (GPLs) reinforcing phase in the matrix, according to three different patterns. Some new and valuable numerical results for the thermo-mechanical buckling analysis of bidirectional porous functionally graded plates with uniform and non-uniform temperature rise were considered by Allahyari *et al.* (2024). An efficient nonlocal finite element model was developed by Belardi *et al.* (2021) to investigate the bending and buckling behavior of functionally graded (FG) nanobeams. Yang (2021) studied axisymmetric bending and free vibration of circular nanoplates with consideration of surface stresses. The effects of the variable nonlocal parameters on the free vibration of power-law and sigmoid functionally graded nanoplates were investigated by Van Vinh (2022) using a simple inverse hyperbolic shear deformation theory incorporating with nonlocal elasticity theory. A novel refined shear deformation beam theory was proposed by Belarbi *et al.* (2022) and applied, for the first time, to investigate the bending behavior of functionally graded sandwich curved beam. The free vibration response of rectangular functionally graded material sandwich nanoplates with simply supported boundary conditions was considered by Daikh *et al.* (2020b).

From the above literature review, it can be seen that dynamic problem of annular/circular nanoplate has not been reported by researchers. The innovation of this article is the use of sinusoidal shear deformation theory for structure modeling, in addition to the use of Visco-Pasternak fractional foundation, as well as the simultaneous consideration of small-scale parameters and surface effect, and the use of numerical solution methods for dynamic analysis of annular/circular nanoplate. For the first time, dynamic response of annular nanoplates with surface effect embedded by visco Pasternak fractional foundation is studied. Size effects are evaluated by modified couple stress theory (MCST) and the surface effects are considered by the Gurtin-Murdoch theory.

2. Formulation

Figs. 1 and 2 show respectively an annular and circular nanoplate under the uniform load. The circular nanoplate has radius of R and thickness of h which the annular one has inner radius of R_i, outer radius of R_o and thickness of h. The nanostructure is on the frictional viscoelastic foundation with spring, damper and shear elements.

In order to model the nanostructure, the SSDT is used and after calculating the strains and stresses, the energies of the structure should be derived. Then, based on Hmailton's principle, the motion equations may be obtained and based on numerical solution, the dynamic deflection will be presented. The flowchart of modelling for this structure is presented in Fig. 3.

The strain energy, U, based on the MCST for an isotropic linear elastic material can be expressed as (Arbabi *et al.* 2017, Azmi *et al.* 2019, Amoli *et al.* 2018)

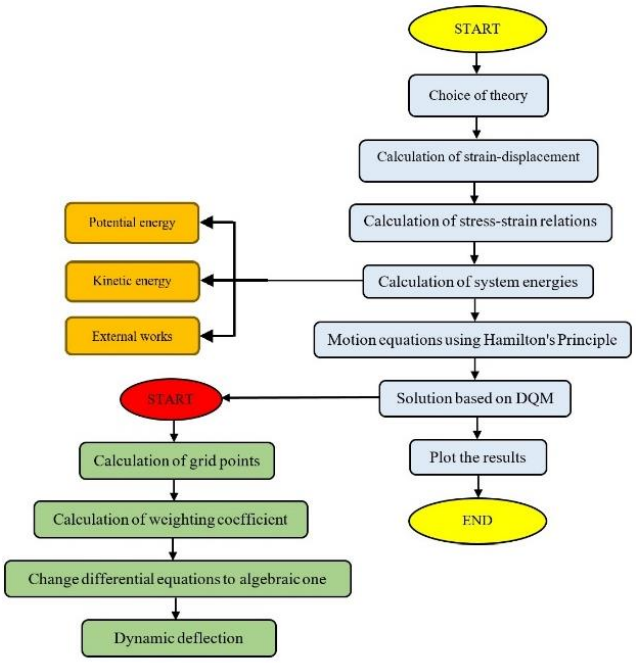

Fig. 3 The flowchart of modelling for the annular/circilar nanoplate

$$U_b = \frac{1}{2}\int_{\Omega}(\sigma_{ij}\varepsilon_{jk} + m_{ij}\chi_{ij})dV \tag{1}$$

where ε_{ij}, χ_{ij}, σ_{ij} and m_{ij} denote the strain, the symmetric curvature, the stress and the deviatoric part of the symmetric couple stress tensors, respectively which can be defined as

$$\varepsilon_{ij} = \frac{1}{2}\left(\frac{\partial u_j}{\partial x_i} + \frac{\partial u_i}{\partial x_j}\right), \tag{2}$$

$$\chi_{ij} = \frac{1}{2}\left(\frac{\partial \theta_i}{\partial x_j} + \frac{\partial \theta_j}{\partial x_i}\right), \theta_i = \frac{1}{2}e_{ijk}\frac{\partial u_k}{\partial x_j} = \frac{1}{2}\nabla\times \mathrm{u}, \tag{3}$$

$$\sigma_{ij} = k\delta_{ij}\varepsilon_{mm} + 2G\varepsilon_{ij}, \tag{4}$$

$$m_{ij} = 2l_0^2 G\chi_{ij}, \tag{5}$$

where l_0 is the material length scale parameter, $e_{ijk}$is the permutation tensor, *K* and G are bulk and shear modulus, respectively which can be expressed in term of Young' modulus (*E*) and Poisson's ratio (ν) as

$$K = \frac{E\nu}{(1+\nu)(1-2\nu)}, \tag{6a}$$

$$G = \frac{E}{2(1+\nu)}. \tag{6b}$$

Based on the modified power-law model, Young's modulus can be described as (Baseri *et al*. 2016, Bilouei *et al*. 2018, Golabchi *et al*. 2018). In this paper, SSDT is used for formulation. It is since, SSDT provides a more accurate representation of the transverse shear strain distribution through the thickness of the structure without the need for shear correction factors, which are often required in polynomial theories. Additionally, SSDT captures the effects of shear deformation more effectively, leading to improved accuracy in predicting deflections and stresses, particularly in thick plates and beams. This theory also avoids the complexity and computational burden associated with higher-order polynomial functions, making it a more efficient choice for certain applications.

Based on Sinusoidal Shear Deformation theory for axisymmetric buckling case, $u = [U, V, W]$ is the displacement vector that is defined as follows (Keshtegar *et al*. 2018, 2020a, b, c):

$$U(r,z) = u(r) - z\frac{dw_b(r)}{dr} + f(z)\frac{dw_s(r)}{dr}, \tag{7a}$$

$$V(r,z) = 0, \tag{7b}$$

$$W(r,z) = w_b(r) + w_s(r), \tag{7c}$$

where *u*, w_b and w_s are mid-plane axial, transverse bending and transverse shear displacements, respectively and $f(z) = \frac{h}{\pi}\left[sin(\frac{\pi z}{h})\right]$. Substituting Eqs. (8)-(10) into Eq. (2), the non-zero components of strain tensor are (Taherifar *et al*. 2020, 2021, Kolahchi 2017, Zamanian *et al*. 2017)

$$\varepsilon_{rr} = \frac{\partial}{\partial r}u(r) - z.\frac{\partial^2}{\partial r^2}w_b(r) + f(z).\frac{\partial^2}{\partial r^2}w_s(r), \tag{8a}$$

$$\varepsilon_{\theta\theta} = \frac{u(r)}{r} - \frac{z}{r}.\frac{\partial}{\partial r}w_b(r) + \frac{f(z)}{r}w_s(r), \tag{8b}$$

$$\varepsilon_{rz} = \frac{\partial w_s(r)}{\partial r} + \left(\frac{\partial f(z)}{\partial z}\right)\left(\frac{\partial w_s(r)}{\partial r}\right). \tag{8c}$$

Substituting Eqs. (9a)-(9c) into Eq. (3), the non-zero components of strain tensor are

$$\begin{aligned}\chi_{r\theta} = &-\left(\frac{\partial^2 w_b(r)}{\partial r^2}\right) + \frac{1}{2}\left(\frac{\partial f(z)}{\partial z}\right)\left(\frac{\partial^2 w_s(r)}{\partial r^2}\right)\\ &-\frac{1}{2}\left(\frac{\partial^2 w_s(r)}{\partial r^2}\right) + \frac{1}{r}\left(\frac{\partial w_b(r)}{\partial r}\right)\\ &-\frac{1}{2r}\left(\frac{\partial f(z)}{\partial z}\right)\left(\frac{\partial w_s(r)}{\partial r}\right) - \frac{1}{2r}\left(\frac{\partial w_s(r)}{\partial r}\right),\end{aligned} \tag{9a}$$

$$\chi_{\theta z} = \frac{1}{2}\left(\frac{\partial^2 f(z)}{\partial z^2}\right)\left(\frac{\partial w_s(r)}{\partial r}\right). \tag{9b}$$

Substituting Eqs. (9a)-(9c) into Eq. (4), the non-zero components of stress tensor are

$$\begin{Bmatrix}\sigma_{rr}^b\\ \sigma_{\theta\theta}^b\\ \sigma_{rz}^b\end{Bmatrix} = \begin{bmatrix}Q_{11}^b & Q_{12}^b & 0\\ Q_{21}^b & Q_{22}^b & 0\\ 0 & 0 & Q_{66}^b\end{bmatrix}\begin{Bmatrix}\varepsilon_{rr}\\ \varepsilon_{\theta\theta}\\ \varepsilon_{rz}\end{Bmatrix} + \begin{Bmatrix}\frac{c_{13}}{c_{33}}\\ \frac{c_{23}}{c_{33}}\\ 0\end{Bmatrix}\sigma_{zz}, \tag{10a}$$

$$\begin{Bmatrix}\sigma_{rr}^s\\ \sigma_{\theta\theta}^s\end{Bmatrix} = \begin{bmatrix}Q_{11}^s & Q_{12}^s\\ Q_{21}^s & Q_{22}^s\end{bmatrix}\begin{Bmatrix}\varepsilon_{rr}\\ \varepsilon_{\theta\theta}\end{Bmatrix}, \tag{10b}$$

$$\sigma_{zz} = \begin{pmatrix}\left(\frac{\partial}{\partial r}\sigma_{rz}^s + \frac{1}{r}\frac{\partial}{\partial\theta}\sigma_{\theta z}^s - \rho_s\frac{\partial^2 w_b(r,t)}{\partial t^2}\right)\\ -\rho_s\frac{\partial^2 w_s(r,t)}{\partial t^2}\end{pmatrix}}{h}z, \tag{10c}$$

$$\sigma_{rz}^{s}=\tau\left(\frac{\partial w_b(x,t)}{\partial r}+\frac{\partial w_s(x,t)}{\partial r}\right), \tag{10d}$$

$$\sigma_{rz}^{s}=\tau\left(\frac{\partial w_b(x,t)}{\partial r}+\frac{\partial w_s(x,t)}{\partial r}\right). \tag{10e}$$

$$\sigma_{rr}^{b}=\frac{E}{1-\nu^2}\begin{pmatrix}\left(\frac{du}{dr}-z\frac{d^2w_b}{dr^2}+f(z)\frac{d^2w_s}{dr^2}\right)\\+\nu\left(\frac{u}{r}-\frac{z}{r}\frac{dw_b}{dr}+\frac{f(z)}{r}\frac{dw_s}{dr}\right)\end{pmatrix}, \tag{11a}$$

$$\sigma_{\theta\theta}^{b}=\frac{E}{1-\nu^2}\begin{pmatrix}\nu\left(\frac{du}{dr}-z\frac{d^2w_b}{dr^2}+f(z)\frac{d^2w_s}{dr^2}\right)\\+\left(\frac{u}{r}-\frac{z}{r}\frac{dw_b}{dr}+\frac{f(z)}{r}\frac{dw_s}{dr}\right)\end{pmatrix}, \tag{11b}$$

$$\sigma_{rz}^{b}=\frac{E}{2(1+\nu)}\left(\frac{dw_s}{dr}+\frac{df(z)}{dz}\frac{dw_s}{dr}\right). \tag{11c}$$

Substituting Eqs. (8a)-(8c) into Eq. (5), the non-zero components of deviatoric part of the symmetric couple stress tensors are

$$\begin{aligned}m_{r\theta}=2l_0G\Bigg(&-\frac{d^2w_b}{dr^2}+\frac{1}{2}\frac{df(z)}{dz}\frac{d^2w_s}{dr^2}-\frac{1}{2}\frac{d^2w_s}{dr^2}\\&+\frac{1}{r}\frac{dw_b}{dr}+\frac{1}{2r}\frac{dw_s}{dr}-\frac{1}{2r}\frac{df(z)}{dz}\frac{dw_s}{dr}\Bigg),\end{aligned} \tag{12a}$$

$$m_{z\theta}=2l_0G\left(\frac{1}{2}\frac{d^2f(z)}{dz^2}\frac{dw_s}{dr}\right). \tag{12b}$$

Substituting Eqs. (8) and (9) into Eq. (1) yields

$$\begin{aligned}U_b=\frac{1}{2}\int_{\Omega}\Bigg[&N_r\left(\frac{du}{dr}+\frac{1}{2}\left(\frac{dw_b}{dr}+\frac{dw_s}{dr}\right)^2\right)\\&-M_{rb}\frac{d^2w_b}{dr^2}+M_{rs}\frac{d^2w_s}{dr^2}+\frac{N_\theta u}{r}-\frac{M_{\theta b}}{r}\frac{dw_b}{dr}\\&+\frac{M_{\theta s}}{r}\frac{dw_s}{dr}+N_{rz}\frac{dw_s}{dr}+Q_{rz}\frac{dw_s}{dr}\\&+P_{r\theta}\left(-\frac{d^2w_b}{dr^2}-\frac{1}{2}\frac{d^2w_s}{dr^2}+\frac{1}{r}\frac{dw_b}{dr}+\frac{1}{2r}\frac{dw_s}{dr}\right)\\&+Y_{r\theta}\left(+\frac{1}{2}\frac{d^2w_s}{dr^2}-\frac{1}{2r}\frac{dw_s}{dr}\right)\\&+T_{z\theta}\left(\frac{1}{2}\frac{dw_s}{dr}\right)\Bigg]rdrd\theta dz,\end{aligned} \tag{13}$$

where the stress resultants and couple resultants are

$$(N_r,M_{rb},M_{rs})=\int_{-h/2}^{h/2}\sigma_{rr}(1,z,f(z))dz, \tag{14a}$$

$$(N_\theta,M_{\theta b},M_{\theta s})=\int_{-h/2}^{h/2}\sigma_{\theta\theta}(1,z,f(z))dz, \tag{14b}$$

$$(N_{rz},Q_{rz})=\int_{-h/2}^{h/2}\sigma_{rz}\left(1,\frac{df(z)}{dz}\right)dz, \tag{14c}$$

$$(P_{r\theta},Y_{r\theta})=\int_{-h/2}^{h/2}m_{r\theta}\left(1,\frac{df(z)}{dz}\right)dz, \tag{14d}$$

$$T_{z\theta}=\int_{-h/2}^{h/2}m_{z\theta}\frac{d^2f(z)}{dz^2}dz, \tag{14e}$$

Substituting Eqs. (8a)-(11b) into Eqs. (14a)-(14e), the stress resultants can be expanded as

$$\begin{aligned}N_{rr}=&\int_{-\frac{h}{2}}^{\frac{h}{2}}\sigma_{rr}^{b}dz+\sigma_{rr}^{b}\big|_{z=\frac{h}{2}}+\sigma_{rr}^{b}\big|_{z=-\frac{h}{2}}=\\&A_{11}\frac{\partial u(r,t)}{\partial r}-(B_{11}-B_{13}^{s})\frac{\partial^2w_b(r,t)}{\partial r^2}+\\&(F_{11}+B_{13}^{s})\frac{\partial^2w_s(r,t)}{\partial r^2}+A_{12}\frac{u(r,t)}{r}-\\&\frac{B_{12}}{r}\frac{\partial w_b(r,t)}{\partial r}+\frac{F_{12}}{r}\frac{\partial w_s(r,t)}{\partial r},\end{aligned} \tag{15a}$$

$$\begin{aligned}M_{rb}=&\int_{-\frac{h}{2}}^{\frac{h}{2}}\sigma_{rr}^{b}zdz+\sigma_{rr}^{b}z\big|_{z=\frac{h}{2}}+\sigma_{rr}^{b}z\big|_{z=-\frac{h}{2}}=\\&B_{11}\frac{\partial u(r,t)}{\partial r}-(D_{11}-D_{13}^{s})\frac{\partial^2w_b(r,t)}{\partial r^2}+\\&(H_{11}+D_{13}^{s})\frac{\partial^2w_s(r,t)}{\partial r^2}+B_{12}\frac{u(r,t)}{r}-\\&\frac{D_{12}}{r}\frac{\partial w_b(r,t)}{\partial r}+\frac{H_{12}}{r}\frac{\partial w_s(r,t)}{\partial r},\end{aligned} \tag{15b}$$

$$\begin{aligned}M_{rs}=&\int_{-\frac{h}{2}}^{\frac{h}{2}}\sigma_{rr}^{b}f(z)dz+\sigma_{rr}^{b}f(z)\big|_{z=\frac{h}{2}}+\sigma_{rr}^{b}f(z)\big|_{z=-\frac{h}{2}}=\\&F_{11}\frac{\partial u(r,t)}{\partial r}-(H_{11}-H_{13}^{s})\frac{\partial^2w_b(r,t)}{\partial r^2}+\\&(I_{11}+H_{13}^{s})\frac{\partial^2w_s(r,t)}{\partial r^2}+F_{12}\frac{u(r,t)}{r}-\\&\frac{H_{12}}{r}\frac{\partial w_b(r,t)}{\partial r}+\frac{I_{12}}{r}\frac{\partial w_s(r,t)}{\partial r},\end{aligned} \tag{15c}$$

$$\begin{aligned}N_\theta=&\nu\left(A\frac{du(r,t)}{dr}-B\frac{d^2w_b(r,t)}{dr^2}+F\frac{d^2w_s(r,t)}{dr^2}\right)\\&+A\frac{u(r,t)}{r}-\frac{B}{r}\frac{dw_b(r,t)}{dr}+\frac{F}{r}\frac{dw_s(r,t)}{dr}\end{aligned} \tag{15d}$$

$$\begin{aligned}M_{\theta b}=&\int_{-\frac{h}{2}}^{\frac{h}{2}}\sigma_{\theta\theta}^{b}zdz+\sigma_{\theta\theta}^{b}z\big|_{z=\frac{h}{2}}+\sigma_{\theta\theta}^{b}z\big|_{z=-\frac{h}{2}}=\\&B_{21}\frac{\partial u(r,t)}{\partial r}-(D_{21}-D_{23}^{s})\frac{\partial^2w_b(r,t)}{\partial r^2}+\\&(H_{21}+D_{23}^{s})\frac{\partial^2w_s(r,t)}{\partial r^2}+B_{22}\frac{u(r,t)}{r}-\\&\frac{D_{22}}{r}\frac{\partial w_b(r,t)}{\partial r}+\frac{H_{22}}{r}\frac{\partial w_s(r,t)}{\partial r}\end{aligned} \tag{15e}$$

$$\begin{aligned}M_{\theta s}=&\int_{-\frac{h}{2}}^{\frac{h}{2}}\sigma_{\theta\theta}^{b}f(z)dz+\sigma_{\theta\theta}^{b}f(z)\big|_{z=\frac{h}{2}}+\sigma_{\theta\theta}^{b}f(z)\big|_{z=-\frac{h}{2}}\\&=F_{21}\frac{\partial u(r,t)}{\partial r}-(H_{21}-H_{23}^{s})\frac{\partial^2w_b(r,t)}{\partial r^2}+\\&(I_{21}+H_{23}^{s})\frac{\partial^2w_s(r,t)}{\partial r^2}+F_{22}\frac{u(r,t)}{r}-\\&\frac{H_{22}}{r}\frac{\partial w_b(r,t)}{\partial r}+\frac{I_{22}}{r}\frac{\partial w_s(r,t)}{\partial r}\end{aligned} \tag{15f}$$

$$\begin{aligned}N_{rz}=&\int_{-\frac{h}{2}}^{\frac{h}{2}}\sigma_{rz}^{b}dz+\sigma_{rz}^{b}\big|_{z=\frac{h}{2}}+\sigma_{rz}^{b}\big|_{z=-\frac{h}{2}}=\\&(A_{66}+\tau)\frac{\partial w_s(r,t)}{\partial r}+(J_{66}+\tau)\frac{\partial w_s(r,t)}{\partial r}.\end{aligned} \tag{15g}$$

$$Q_{rz}=\int_{-\frac{h}{2}}^{\frac{h}{2}}\sigma_{rz}^{b}f(z)dz+\sigma_{rz}^{b}f(z)\big|_{z=\frac{h}{2}}+\sigma_{rz}^{b}f(z)\big|_{z=-\frac{h}{2}}= \tag{15h}$$

$$(J_{66}+\tau)\frac{\partial w_s(r,t)}{\partial r}+(L_{66}+\tau)\frac{\partial w_s(r,t)}{\partial r}.$$

$$P_{r\theta}=l_0(1-\nu)\left(-A\frac{d^2w_b(r,t)}{dr^2}+\frac{J}{2}\frac{d^2w_s(r,t)}{dr^2}-\frac{A}{2}\frac{d^2w_s(r,t)}{dr^2}+\frac{A}{r}\frac{dw_b(r,t)}{dr}+\frac{A}{2r}\frac{dw_s(r,t)}{dr}-\frac{J}{2r}\frac{dw_s(r,t)}{dr}\right) \quad (15i)$$

$$Y_{r\theta}=l_0(1-\nu)\left(-J\frac{d^2w_b(r,t)}{dr^2}+\frac{L}{2}\frac{d^2w_s(r,t)}{dr^2}-\frac{M}{2}\frac{d^2w_s(r,t)}{dr^2}+\frac{M}{r}\frac{dw_b(r,t)}{dr}+\frac{M}{2r}\frac{dw_s(r,t)}{dr}-\frac{L}{2r}\frac{dw_s(r,t)}{dr}\right), \quad (15j)$$

$$T_{z\theta}=l_0(1-\nu)\frac{M}{2}\frac{dw_s(r,t)}{dr}, \quad (15k)$$

where

$$\begin{pmatrix}A,B,D,F,H,\\I,J,L,M\end{pmatrix}=\frac{E}{1-\nu^2}\int_{-h/2}^{h/2}\begin{pmatrix}1,z,z^2,f(z)\\,zf(z),f(z)^2,\frac{df(z)}{dz}\\,\left(\frac{df(z)}{dz}\right)^2,\frac{d^2f(z)}{dz^2}\end{pmatrix}dz. \quad (16a)$$

$$A_{11}=\int_{-\frac{h}{2}}^{\frac{h}{2}}Q_{11}^b dz+Q_{11}^s|_{z=\frac{h}{2}}+Q_{11}^s|_{z=-\frac{h}{2}} \quad (16b)$$

$$A_{12}=\int_{-\frac{h}{2}}^{\frac{h}{2}}Q_{12}^b dz+Q_{12}^s|_{z=\frac{h}{2}}+Q_{12}^s|_{z=-\frac{h}{2}} \quad (16c)$$

$$A_{22}=\int_{-\frac{h}{2}}^{\frac{h}{2}}Q_{22}^b dz+Q_{22}^s|_{z=\frac{h}{2}}+Q_{22}^s|_{z=-\frac{h}{2}} \quad (16d)$$

$$A_{66}=\int_{-\frac{h}{2}}^{\frac{h}{2}}c_{55}dz+c_{11}^s|_{z=\frac{h}{2}}+c_{11}^s|_{z=-\frac{h}{2}} \quad (16e)$$

$$B_{11}=\int_{-\frac{h}{2}}^{\frac{h}{2}}Q_{11}^b z dz+Q_{11}^s z|_{z=\frac{h}{2}}+Q_{11}^s z|_{z=-\frac{h}{2}} \quad (16f)$$

$$B_{12}=\int_{-\frac{h}{2}}^{\frac{h}{2}}Q_{12}^b z dz+Q_{12}^s z|_{z=\frac{h}{2}}+Q_{12}^s z|_{z=-\frac{h}{2}} \quad (16g)$$

$$B_{22}=\int_{-\frac{h}{2}}^{\frac{h}{2}}Q_{22}^b z dz+Q_{22}^s z|_{z=\frac{h}{2}}+Q_{22}^s z|_{z=-\frac{h}{2}} \quad (16h)$$

$$D_{11}=\int_{-\frac{h}{2}}^{\frac{h}{2}}Q_{11}^b z^2 dz+Q_{11}^s z^2|_{z=\frac{h}{2}}+Q_{11}^s z^2|_{z=-\frac{h}{2}} \quad (16i)$$

The normal interface pressure between the structure and frictional viscoelastic torsional foundations is

$$F_V=k_w w+c_d\dot{w}-k_g\left(\frac{\partial^2 w}{\partial x^2}+\frac{\partial^2 w}{R(x)^2\,\partial\theta^2}\right) \quad (17)$$

$$F_f=\mu_f F_V, \quad (18)$$

$$F_T=k_{t1}\gamma-\frac{\partial}{\partial x}\left(k_{t2}\frac{\partial\gamma}{\partial x}\right)\overrightarrow{\gamma=\frac{\partial v}{\partial x}}F_T=k_{t1}\frac{\partial v}{\partial x}-k_{t2}\frac{\partial^3 v}{\partial x^3}, \quad (19)$$

In order to obtain the governing equations, Hamilton's principle is used as

$$\int_0^t(\delta\Pi)dt=\int_0^t-(\delta U_b+\delta W_e+\delta W_r)dt=0 \quad (20)$$

where δ is variation operator, Π is the total potential energy of the nanostructure. Substituting Eqs. (13), (17) and (19) into Eq. (20) yields

$$\begin{aligned}2\pi\int\Bigg[&rN_r\left(\frac{d\delta u}{dr}+\frac{dw_b}{dr}\frac{d\delta w_b}{dr}+\frac{dw_s}{dr}\frac{d\delta w_s}{dr}+\frac{dw_s}{dr}\frac{d\delta w_b}{dr}+\frac{d\delta w_s}{dr}\frac{dw_b}{dr}\right)\\&+N_\theta(\delta u)+rN_{rz}\left(\frac{d\delta w_s}{dr}\right)+rQ_{rz}\left(\frac{d\delta w_s}{dr}\right)\\&-rM_{rb}\left(\frac{d^2\delta w_b}{dr^2}\right)+rM_{rs}\left(\frac{d^2\delta w_s}{dr^2}\right)\\&-M_{\theta b}\left(\frac{d\delta w_b}{dr}\right)+M_{\theta s}\left(\frac{d\delta w_s}{dr}\right)\\&+rP_{r\theta}\left(-\frac{d^2\delta w_b}{dr^2}-\frac{1}{2}\frac{d^2\delta w_s}{dr^2}+\frac{1}{r}\frac{d\delta w_b}{dr}+\frac{1}{2r}\frac{d\delta w_s}{dr}\right)\\&+rY_{r\theta}\left(\frac{1}{2}\frac{d^2\delta w_s}{dr^2}-\frac{1}{2r}\frac{d\delta w_s}{dr}\right)\\&+rT_{z\theta}\left(\frac{1}{2}\frac{d\delta w_s}{dr}\right)+q_{fractional}\,r\,(\delta w_b+\delta w_s)\\&+(N_1+N_2)u\Bigg]dr=0\end{aligned} \quad (21)$$

Integrating the parts from the above relation, and collecting the coefficients of δu, δwb, δws, the governing equilibrium equations can be obtained as follows

$$\delta U:\frac{1}{r}\left\{\frac{\partial}{\partial r}[r.N_{rr}(r)]-N_{\theta\theta}(r)\right\}=0, \quad (22a)$$

$$\delta w_b:\frac{1}{r}\left\{\begin{matrix}\frac{\partial^2}{\partial r^2}[r.M_{rb}(r)]-\frac{\partial}{\partial r}M_{\theta b}(r)+\\\frac{\partial}{\partial r}\left[N_{rm}.r(\frac{\partial}{\partial r}[w_b(r)+w_s(r)])\right]+\\N_{\theta m}\frac{\partial}{\partial r}w_b(r)+\frac{\partial}{\partial r}P_{r\theta}\end{matrix}\right\}-q_{fractional}=F \quad (22b)$$

$$\delta w_s:\frac{1}{r}\left\{\begin{matrix}\frac{\partial}{\partial r}M_{\theta s}(r)+\frac{\partial}{\partial r}[r.N_{rz}(r)]+\\\frac{\partial}{\partial r}\left[N_{rm}.r(\frac{\partial}{\partial r}[w_b(r)+w_s(r)])\right]+\\N_{\theta m}\frac{\partial}{\partial r}w_s(r)+\frac{\partial}{\partial r}[r.Q_{rz}]-\\\frac{\partial^2}{\partial r^2}[r.M_{rs}(r)]+\frac{1}{2}\frac{\partial}{\partial r}P_{r\theta}-\frac{1}{2}\frac{\partial}{\partial r}Y_{r\theta}\end{matrix}\right\}+\frac{1}{2}\frac{\partial^2}{\partial r^2}P_{r\theta}-\frac{1}{2}\frac{\partial^2}{\partial r^2}Y_{r\theta}+\frac{1}{2}\frac{\partial}{\partial r}T_{z\theta}-q_{fractional}=F \quad (22c)$$

where N_r^M and N_θ^M are prebuckling stress resultants in the radial and circumferential directions, respectively.

3. Solution method

Nowadays, DQM is a numerical solution method. Used to solve complex differentiation equations. In this method, for differentiation equations, they are first converted to algebraic equations using chebyshev polynomile and weighting coefficient's. Then, with the help of border conditions, it solves them (Bakhshandeh Amnieh *et al*. 2018, Hajmohammad *et al*. 2018a, b, 2019a, b, c, 2021, Kolahchi *et al*. 2013, 2015, 2016a, b, Kolahchi and Moniribidgoli 2016)

$$\begin{aligned} f^1(r_i) &= \sum_{j=1}^{N_r} C_{ij}^{(1)} f(r_j)\, for i = 0,\dots,N_r \\ f_r^{(m-1)}(r_i) &= \sum_{j=1}^{N_r} C_{ij}^{(m-1)} f(r_j)\, for i = 1,2,..,N_r m \\ &= 2,3,\dots,N_r - 1 \\ f_r^{(m)}(r_i) &= \sum_{j=1}^{N_r} C_{ij}^{(m)} f(r_j)\, for i = 1,2,..,N_r m \\ &= 2,3,\dots,N_r - 1 \end{aligned} \tag{23}$$

where Nr and ri are the number of grid points and given discrete grid points, respectively, $C_{ij}^{(1)}$ and $C_{ij}^{(m)}$ stand for the respective weighting coefficient related to the first-order and mth-order derivative weighting coefficients, which is obtained as follows

$$\begin{aligned} C_{ij}^{(1)} &= \frac{M^{(1)}(r_i)}{(r_i - r_j)M^{(1)}(r_j)} for i \neq j, i, j = 1,2,\dots,N_r \\ C_{ii}^{(1)} &= \frac{M^{(2)}(r_i)}{2M^{(1)}(r_i)} for i = 1,2,\dots,N_r \\ C_{ij}^{(m-1)} &= \frac{N^{(m-1)}(r_i, r_j)}{M^{(1)}(r_j)} \\ C_{ij}^{(m)} &= \frac{N^{(m)}(r_i, r_j)}{M^{(1)}(r_j)} \end{aligned} \tag{24}$$

where M and N are determined by recurrence relations as follows

$$\begin{aligned} M^{(1)}(r_i) &= \prod_{\substack{k=1 \\ k\neq i}}^{N_r} (r_i, r_k) \\ N^{(m-1)}(r_i, r_j) &= M^{(1)}(r_i)\, C_{ij}^{(m-1)} \\ N^{(m-1)}(r_i, r_i) &= \frac{M^{(m)}(r_i)}{m} \\ N^{(m)}(r_i, r_j) &= \frac{M^{(m)}(r_i) - m\, N^{(m-1)}(r_i, r_j)}{(r_i - r_j)} for i \neq j \end{aligned} \tag{25}$$

For optimal choice to determinate the coordinates of the grid points, well-accepted set is the Gauss-Lobatto-Chebyshev points given for annular and circular nanoplates, respectively, as (Jafarian Arani *et al*. 2016)

$$r_i = \frac{R_o}{2}\left[1 - cos\left(\frac{i-1}{N_r - 1}\right)\pi\right] + R_i \, i = 1,\dots,N_r \tag{26a}$$

$$r = \frac{R}{2}\left[1 - cos\left(\frac{i-1}{N_r - 1}\right)\pi\right] i = 1,\dots,N_r \tag{26b}$$

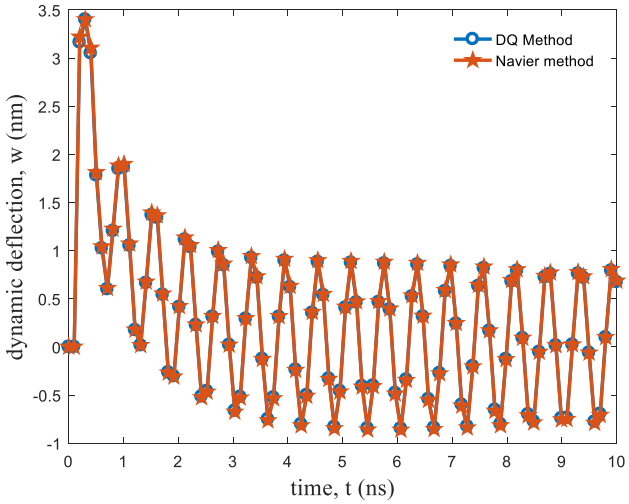

Fig. 4 Dynamic deflection versus time for DQ and Navier methods

By substituting of Eq. (31) into Eqs. (26a)-(26c), the governing differential equations in buckling are rearranged in form of matrix, as:

$$[k_g]P + [K]d = 0 \tag{27}$$

where $y = [u, w_b, w_s]$, b and d indexes are associated to boundary and domain points, respectively, [K] are stiffness and geometrical coefficients, respectively. Finally, using an iterative method and eigenvalue problem, the solution of Eq. (27) yields to the nonlinear bucklingannular/circular nanoplate.

4. Numerical results

Herein, in this section, the effect of various parameters such as: damper constants of fractional, thickness-to-radius ratio, spring constants of fractional foundation, thickness-to- Small scale parameter ratio, Scale parameter to thickness ratio, inner radius and surface effect on the dynamic deflection annular nanoplate are considered.

For validation, since we can not find a paper in the field of this paper exactly, we solved the motion equations with two methods and compared the results. Based on Navier method, steady state solutions to the motion equations which relate to the simply supported boundary conditions can be assumed as Thai and Vo (2013):

$$U(x,t) = u(t)\, cos\left(\frac{m\pi x}{a}\right), \tag{28}$$

$$W_b(x,t) = w_b(t)\, sin\left(\frac{m\pi x}{a}\right), \tag{29}$$

$$W_s(x,t) = w_s(t)\, sin\left(\frac{m\pi x}{a}\right), \tag{30}$$

Substituting and Eqs. (28)-(30) into motion equations and neglecting nonlinear terms yields:

$$([K_L] + \Omega^2[M])\{d_0\} = 0 \tag{31}$$

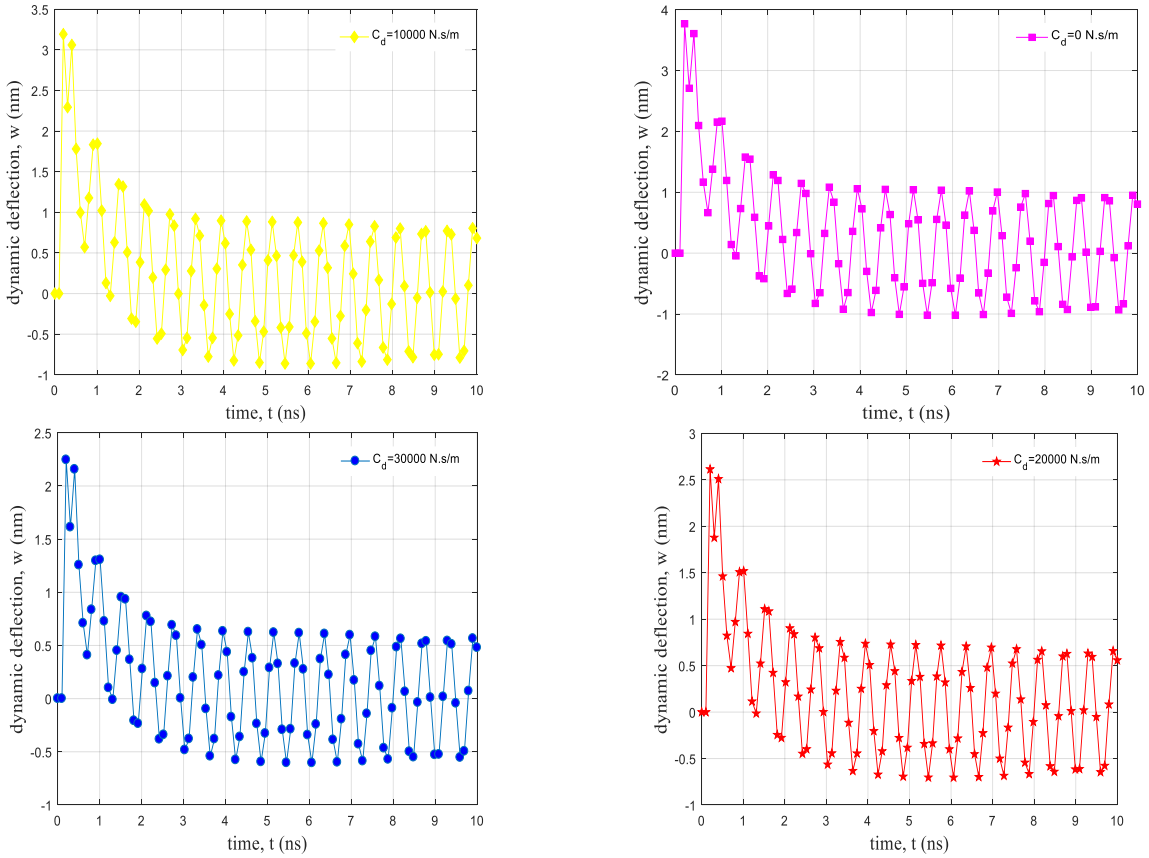

Fig. 5 The effect of damper constants of fractional foundation on the dynamic deflection annular nanoplate

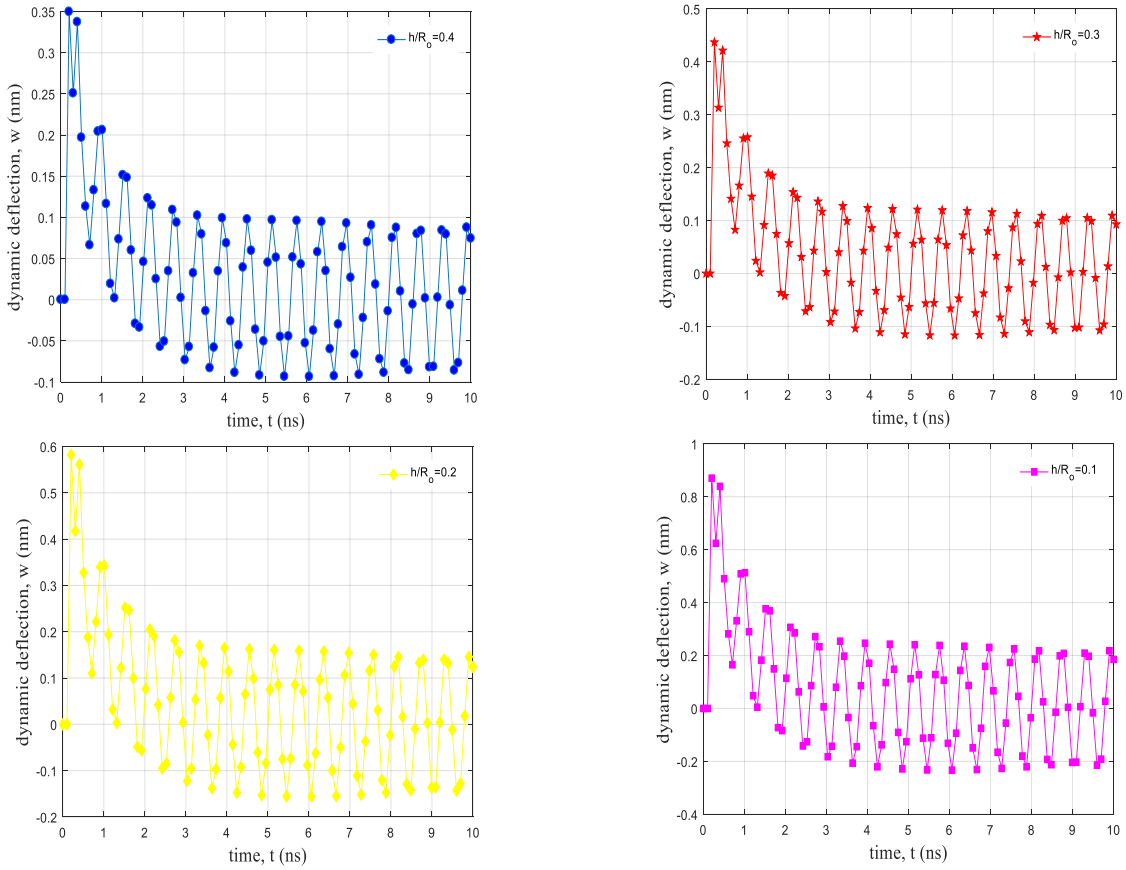

Fig. 6 The ratio of thickness to inner radius effect on the dynamic deflection annular nanoplate

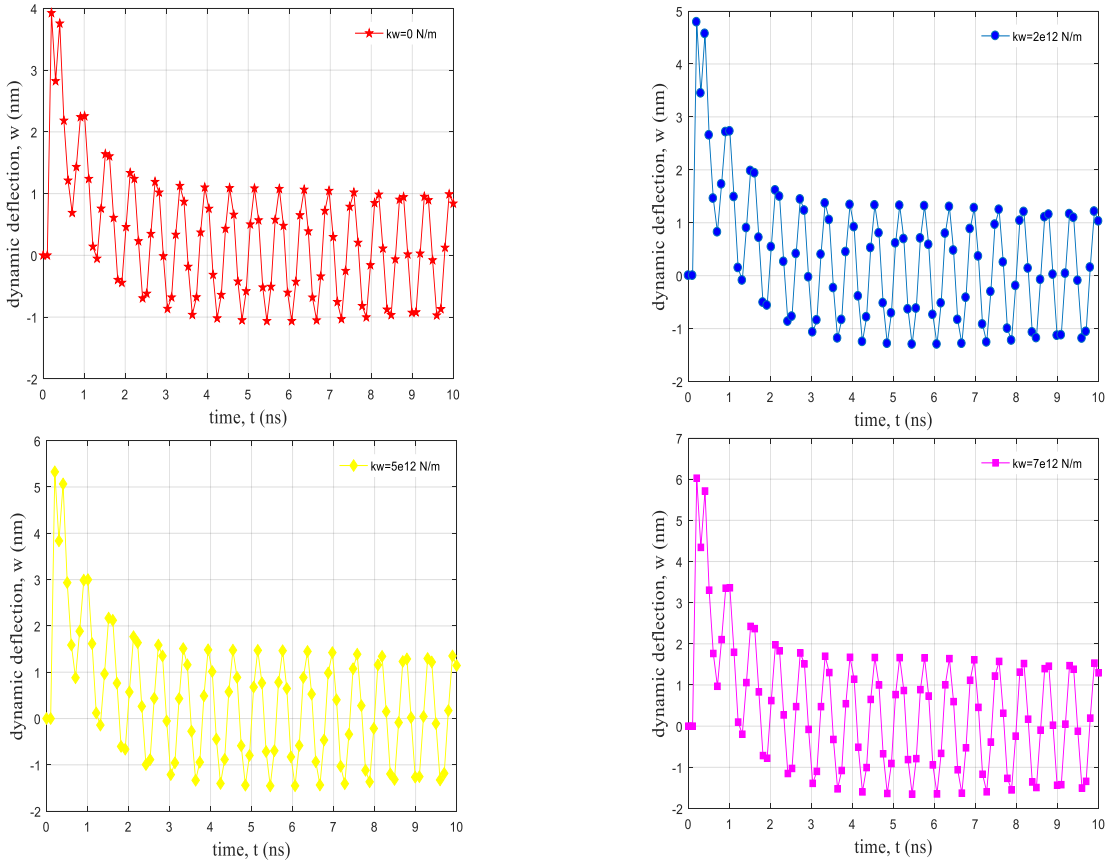

Fig. 7 The effect of spring constants of fractional foundation on the dynamic deflection anuular nanoplate

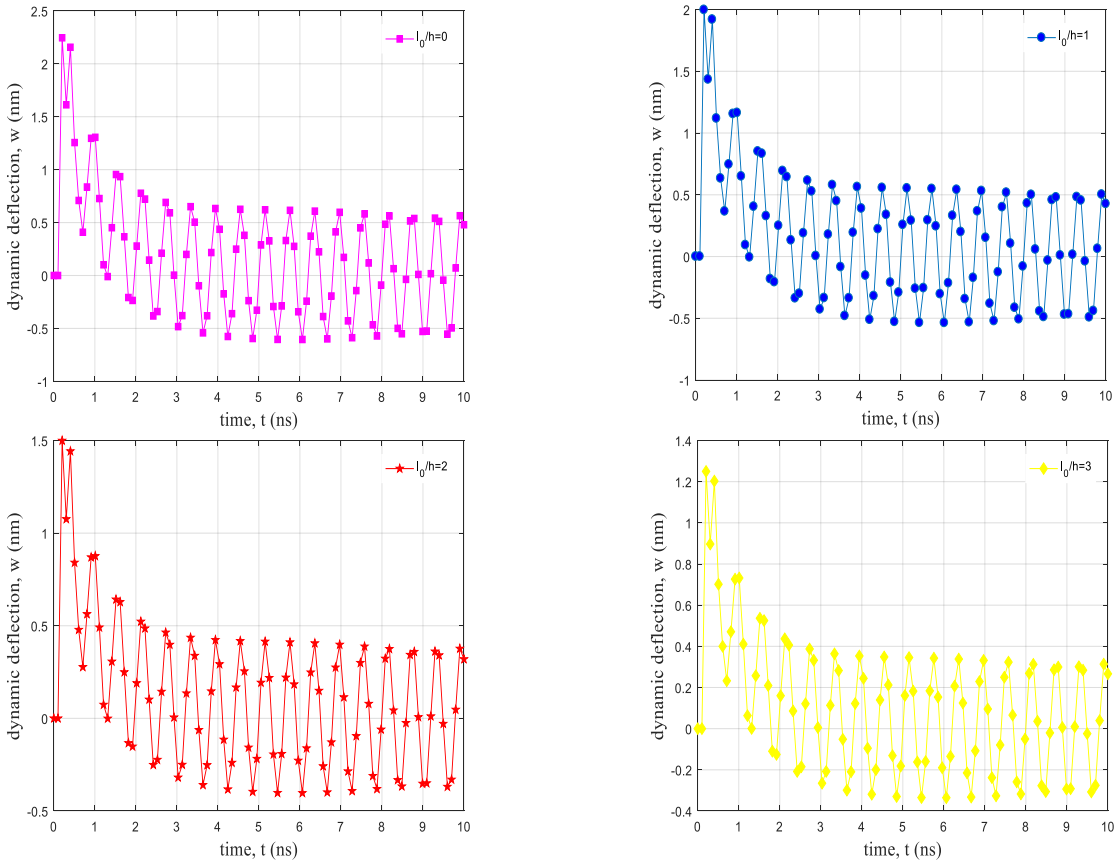

Fig. 8 Scale parameter to thickness ratio on the dynamic deflection anuular nanoplate

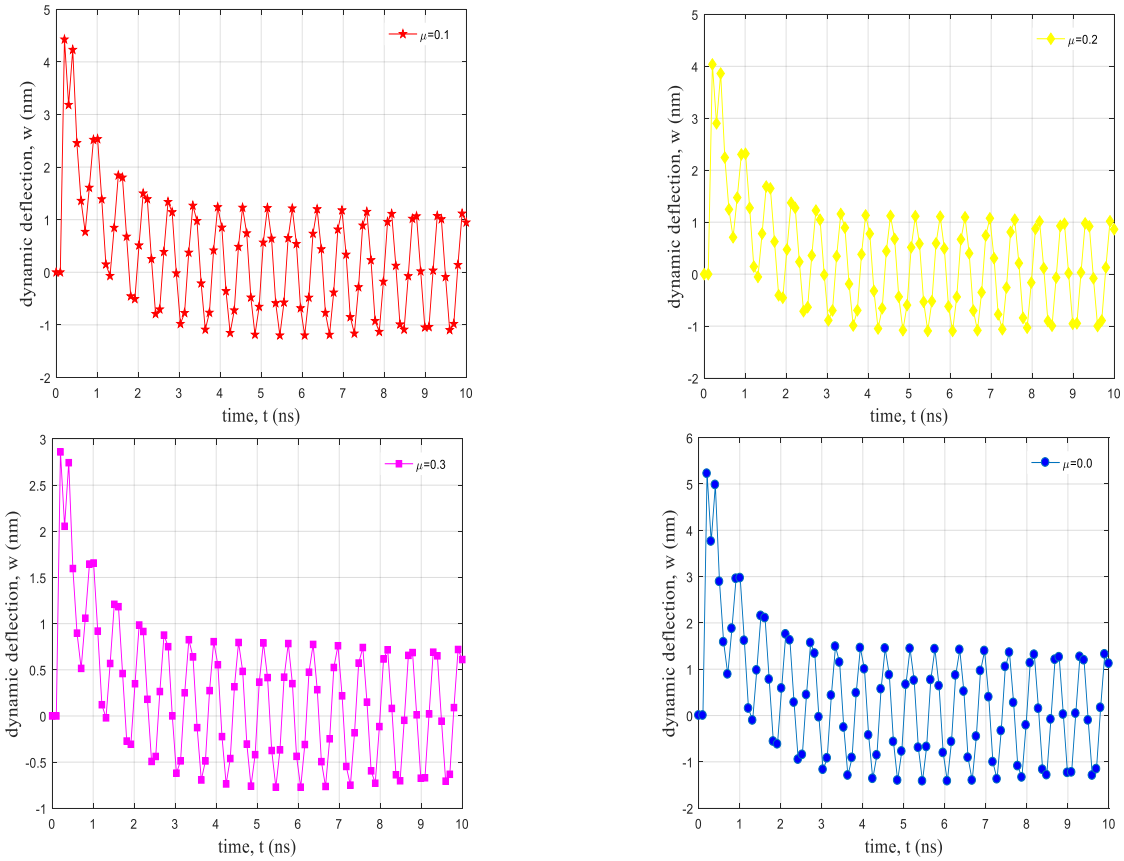

Fig. 9 The effect of fraction factor of fractional foundation on the dynamic deflection annular nanoplate

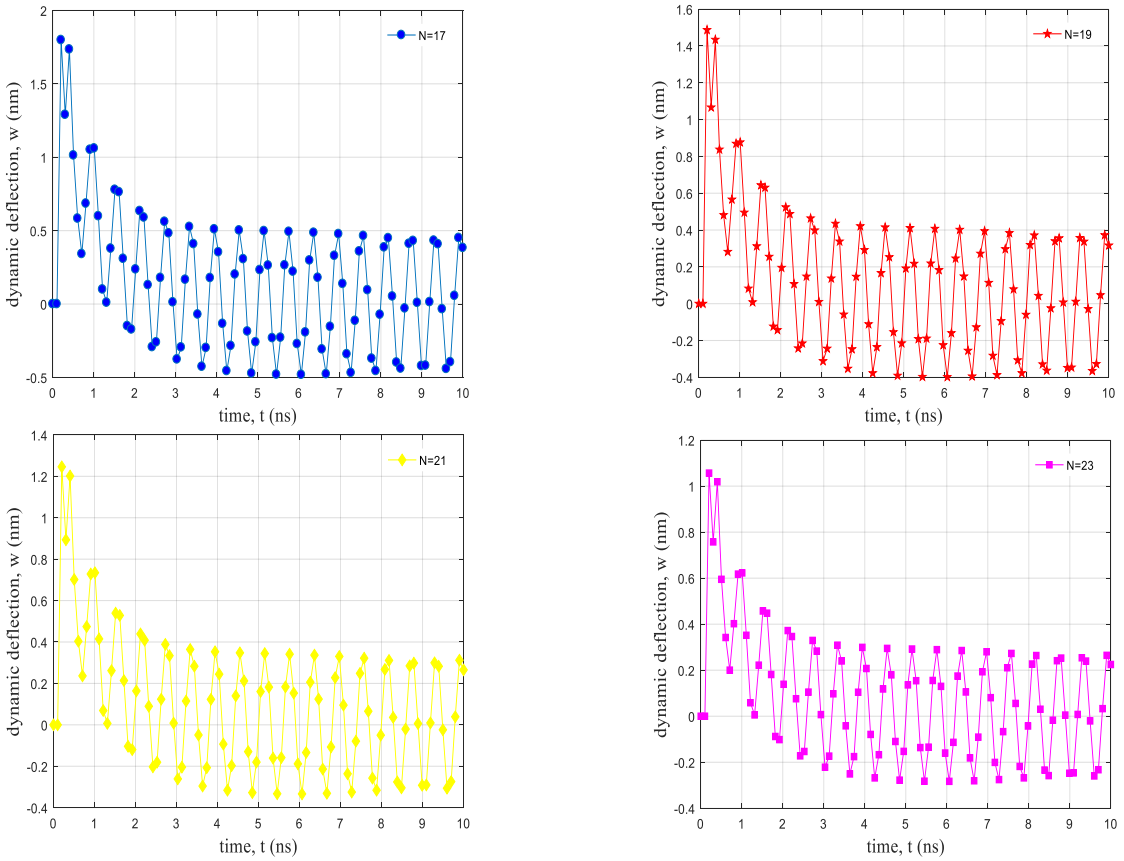

Fig. 10 The convergence points on the dynamic deflectin annular nanoplate

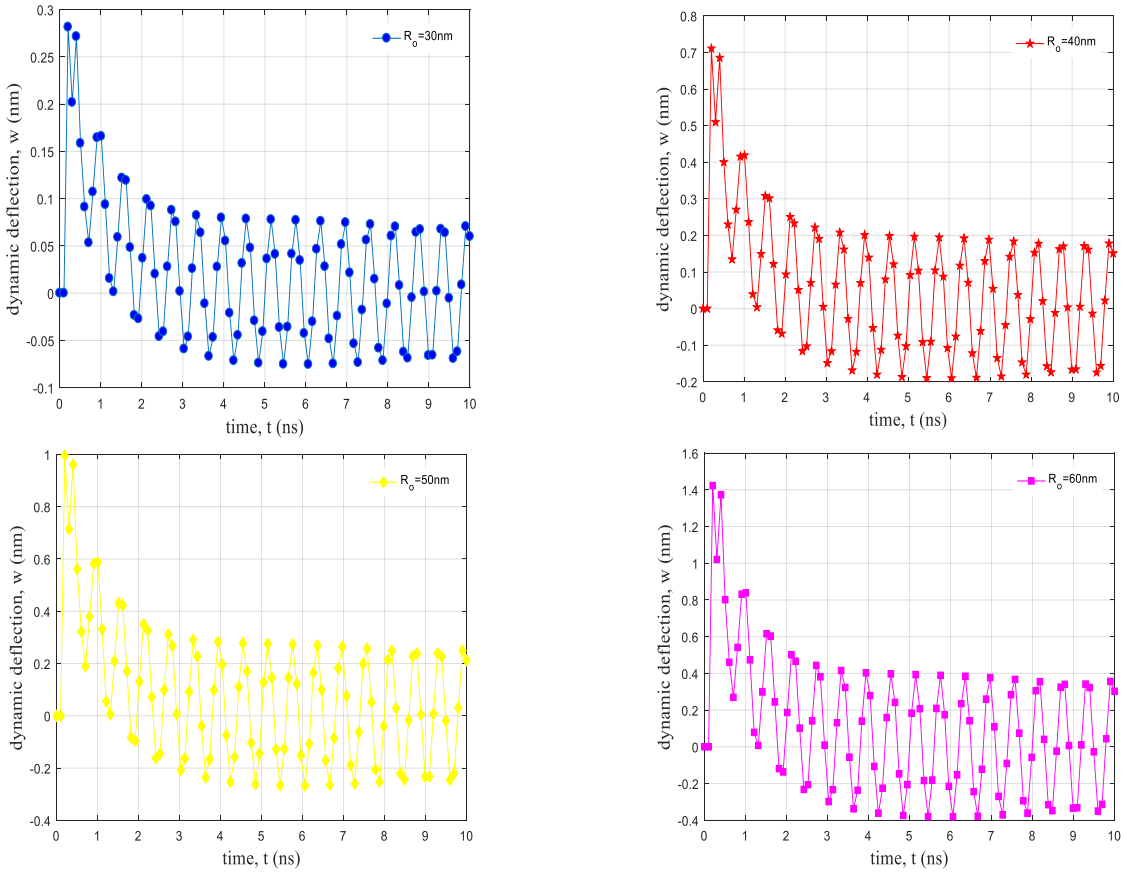

Fig. 11 The inner radius on the dynamic deflection annular nanoplate

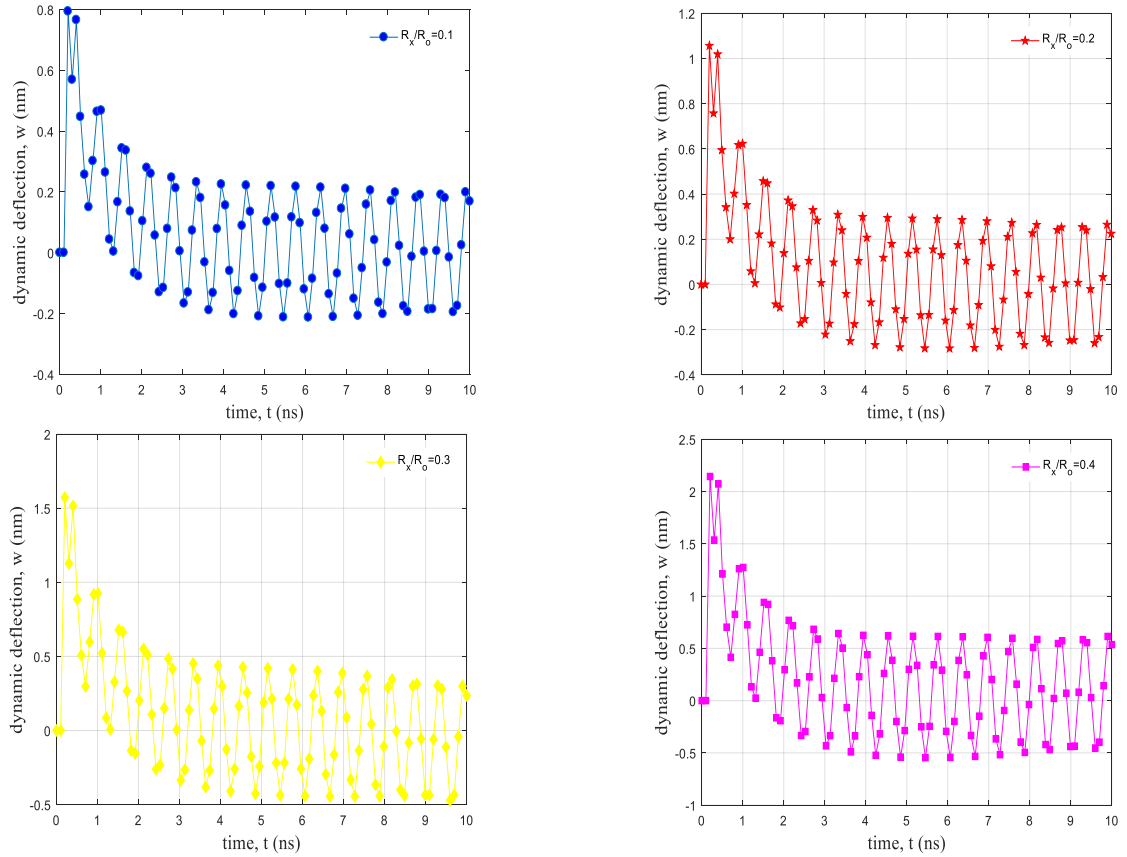

Fig. 12 Ratio of inner to outer radius on the dynamic deflection annular nanoplate

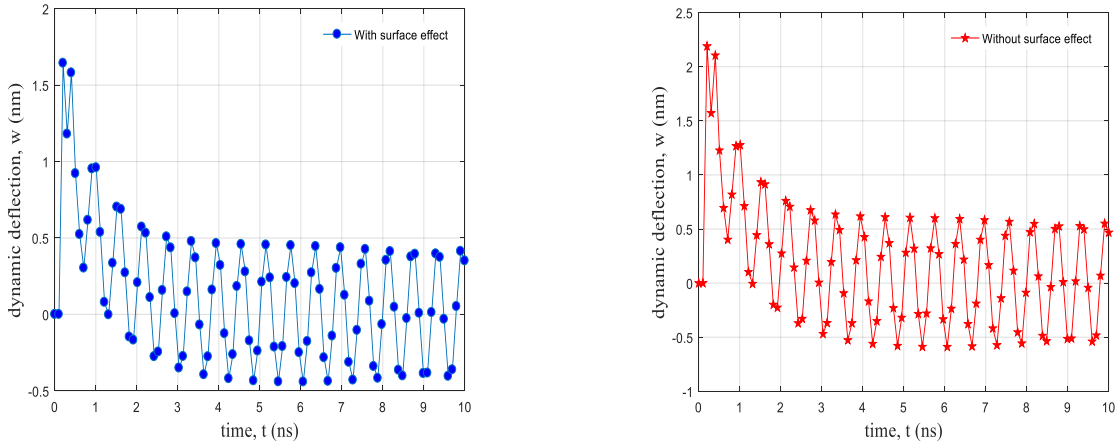

Fig. 13 The surface effect on the dynamic deflection annular nanoplate

By solving Eq. (31) utilizing the problem of eigenvalue, the dynamic deflection of the structure may be determined. According to Fig. 6, numerical and analytical methods (DQm and Navier) have been compared that the results are in good agreement with each other.

In Fig. 5, the effect of damper constants of fractional foundation on the dynamic deflection of annular nanoplate is shown. The dynamic deflection for the annular nanoplate and shear constants of fractional foundation for the circular nanoplate are shown. In general, with increasingthe damp constants of fractional foundation, the dynamic deflection is reducing due to enhance in the resistance against the deformation is decreased.

Fig. 6 illustrates the effect of thickness-to-radius ratio on dynamic deflection versus h/Ro for the annular nanoplate. As seen, with increasing aforementioned ratio, the dynamic deflection is increased due to increasing the stiffness of the nanoplate.

The effect of spring constants of fractional foundation on the dynamic deflection for the annular nanoplate is presented in Fig. 7. As seen, by increasing the spring constants of fractional foundation, the dynamic deflection is increased.

Fig. 8 illustrates the effect of thickness-to- Small scale parameter ratio on the dynamic deflection versus l0/h for the annular nanoplate. As seen, with increasing afore-mentioned ratio, the dynamic deflection is increased due to upgrading the stiffness of the nanoplate.

The effect of fraction factor constants of fractional foundation on the dynamic deflection for the annular nanoplate is presented in Fig. 9. As seen, by increasing thespring constants of fractional foundation, the dynamic deflection is increased.

The Convergence points is presented in Fig. 9. As can be deduced from the graph, convergence has been obt ained for 19 points.

Fig. 11 illustrates the inner radius on the dynamic deflection versus Ro for the annular nanoplates. As seen, with increasing inner radius, the dynamic deflection is increased due to upgrading the stiffness of the nanoplate.

The effect ratio of inner to outer radius on the dynamic deflection for the annular nanoplate is presented in Fig. 12. As seen, by increasing the ratio of inner to outer radius, the dynamic deflection is increased.

Fig. 13 shows the effect of surface on the structure, it can be concluded that considering the effect of surface on the structure dynamic rise of the structure is reduced.

5. Conclusions

Dynamic response of embedded annular nanoplates with surface effect by visco pasternak fractional foundation has been presented in this work. The size effects are captured based on MCST and the governing equations are derived by utilizing sinusoidal shear deformation theory. DQM is adopted as numerical solution procedure to monitor the influence of various constants of Kerr medium, material length scale parameter, geometrical parameters of the nanoplate, effect of surface ratio of inner to outer radius, dynamic deflection of the annular nanoplate. The results show that with increasing aforementioned ratio, the dynamic deflection is increased due to increasing the stiffness of the nanoplate. increasing inner radius, the dynamic deflection is increased due to upgrading the stiffness of the nanoplate. considering the effect of surface on the structure dynamic rise of the structure is reduced. In addition, with enhancing the material length scale parameter-to-thickness ratio and shear constant of Kerr foundation, the effect of spring constants of Kerr foundation on the dynamic deflection will be more considerable.

References

Allahyari, S.M.R., Shokravi, M. and Murmy, T.T. (2024), "Modeling of truncated nanocompositeconical shell structures for dynamic stability response", *Struct. Eng. Mech.*, **91**(3), 325-334. https://doi.org/10.12989/sem.2024.91.3.325.

Allehaibi, A.M. and Zenkour, A.M. (2022), "Magneto-thermoelastic response in an infinite medium with a spherical hole in the context of high order time-derivatives and triple-phase-lag model", *Materials*, **15**(18), 6256. https://doi.org/10.3390/ma15186256.

Arbabi, A., Kolahchi, R. and Rabani Bidgoli, M. (2017),

"Concrete columns reinforced with Zinc Oxide nanoparticles subjected to electric field: buckling analysis", *Wind Struct*., **24**(5), 431-446. https://doi.org/10.12989/was.2017.24.5.431

Amoli, A., Kolahchi, R. and Rabani Bidgoli, M. (2018), "Seismic analysis of AL2O3 nanoparticles-reinforced concrete plates based on sinusoidal shear deformation theory", *Earthq. Struct*. **15**(3), 285-294. https://doi.org/10.12989/eas.2018.15.3.285

Azmi, M., Kolahchi, R. and Rabani Bidgoli, M. (2019), "Dynamic analysis of concrete column reinforced with Sio2 nanoparticles subjected to blast load", *Adv. Concr. Constr*., **7**(1), 51-63. https://doi.org/10.12989/acc.2019.7.1.051

Baseri, V., Jafari, G.S. and Kolahchi, R. (2016), "Analytical solution for buckling of embedded laminated plates based on higher order shear deformation plate theory", *Steel Compos. Struct*., **21**(4), 883-919. https://doi.org/10.12989/scs.2016.21.4.883

Bilouei, B.S., Kolahchi, R., and Bidgoli, M.R. (2018), "Buckling of beams retrofitted with Nano-Fiber Reinforced Polymer (NFRP)", *Comput. Concr*., **18**(6), 1053-106. https://doi.org/10.12989/cac.2016.18.6.1053.

Bakhshandeh Amnieh, H., Zamzam, M.S. and Kolahchi, R. (2018), "Dynamic analysis of non-homogeneous concrete blocks mixed by SiO2 nanoparticles subjected to blast load experimentally and theoretically", *Constr. Build. Mater*., **174**, 633-644. https://doi.org/10.1016/j.conbuildmat.2018.04.140

Baseri, V., Jafari, G.S., Kolahchi, R. (2016), "Analytical solution for buckling of embedded laminated plates based on higher order shear deformation plate theory", *Steel Compos. Struct*., **21**(4), 883-919, http://doi.org/10.12989/scs.2016.21.4.883.

Bahrami, A. and Teimourian, A. (2017), "Small scale effect on vibration and wave power reflection in circular annular nanoplates", *Compos. B. Eng*., **109**(15), 214-226. https://doi.org/10.1016/j.compositesb.2016.09.107

Belarbi, M.O., Houari, M.S.A., Daikh, A.A., Garg, A,. Merzouki, T., Chalak, H.D. and Hirane, H. (2021), "Nonlocal finite element model for the bending and buckling analysis of functionally graded nanobeams using a novel shear deformation theory", *Compos. Struct*., **264**. https://doi.org/10.1016/j.compstruct.2021.113712.

Belarbi, M.O., Houari, M.S.A., Hirane, H., Daikh, A.A. and Bordas, S.P.A. (2022), "On the finite element analysis of functionally graded sandwich curved beams via a new refined higher order shear deformation theory", *Compos. Struct*., **279**, 114715. https://doi.org/10.1016/j.compstruct.2021.114715

Blanc, M. and Touratier, M. (2002), "An efficient and simple refined model for temperature analysis in thin laminated composites", *Compos. Struct*., **77**, 193-205, https://doi.org/10.1016/j.compstruct.2005.07.001.

Bouazza, M. and Zenkour, A.M. (2024), "Hygrothermal environmental effect on free vibration of laminated plates using nth-order shear deformation theory", *Waves Random Complex Med*., **15**, 307-323. https://doi.org/10.1080/17455030.2021.1909173.

Daikh, A.A., Drai, A., Houari, M.S.A. and Eltaher M.A. (2020a), "Static analysis of multilayer nonlocal strain gradient nanobeam reinforced by carbon nanotubes", *Steel Compos. Struct*., **36**(6), 643-656. https://doi.org/10.12989/scs.2020.36.6.643.

Daikh, A.A., Drai, H. and Tounsi, A. (2020b), "On vibration of functionally graded sandwich nanoplates in the thermal environment", *J. Sandw. Struct. Mater*., **23**(6). https://doi.org/10.1177/1099636220909790.

Daikh, A.A., Drai, A., Houari, M.S.A., Eltaher, M.A.J.S. and Structures, C. (2023), "Static analysis of multilayer nonlocal strain gradient nanobeam reinforced by carbon nanotubes", *Adv. Nano Res*., **36**(6), 643-656. http://doi.org/10.12989/anr.2020.36.6.643.

Dau, F., Polit, O. and Touratier, M. (2004), "An efficient C1 finite element with continuity requirements for multilayered/sandwich shell structures", *Comput. Struct*., **82**, 1889-1899. https://doi.org/10.1016/j.compstruc.2003.10.026.

Dau, F., Polit, O. and Touratier, M. (2006), "C^1 plate and shell finite elements for geometrically nonlinear analysis of multilayered structures", *Comput. Struct*., **84**, 1264-1274, https://doi.org/10.1016/j.compstruc.2006.01.031.

Farrokhian, A. (2023), "Buckling response of smart plates reinforced by nanoparticles utilizing analytical method", *Adv. Nano Res*., **35**(1), 1-12. http://doi.org/10.12989/anr.2020.35.1.001.

Farrokhian, A. (2022), "The effect of voltage and nanoparticles on the vibration of sandwich nanocomposite smart plates", *Adv. Nano Res*., **34**(5), 733-742. http://doi.org/10.12989/anr.2020.34.5.733.

Ganapathi, M., Patel, B.P. and Touratier, M. (2004), "Refined finite element for piezoelectric laminated composite beams", *Smart Mater. Struct*., **13**(57). https://doi.org/10.1088/0964-1726/13/4/N04.

Garg, A., Chalak, H.D., Zenkour, A.M., Belarbi, M.O. and Houari, M.S.A. (2020), "A review of available theories and methodologies for the analysis of nano isotropic, nano functionally graded, and CNT reinforced nanocomposite structure", *Arch. Comput. Meth. Eng*., **29**, 2237-2270. https://doi.org/10.1007/s11831-021-09652-0.

Golabchi, H., Kolahchi, R. and Rabani Bidgoli, M. (2018), "Vibration and instability analysis of pipes reinforced by SiO2 nanoparticles considering agglomeration effects", *Comput. Concr*., **21**, 431-440. https://doi.org/10.12989/cac.2018.21.4.431.

Hajmohammad, M.H., Azizkhani, M.B. and Kolahchi, R. (2018a), "Multiphase nanocomposite viscoelastic laminated conical shells subjected to magneto-hygrothermal loads: Dynamic buckling analysis", *Int. J. Mech. Sci*., **137**, 205-213 https://doi.org/10.1016/j.ijmecsci.2018.01.026.

Hajmohammad, M.H., Maleki, M. and Kolahchi, R. (2018b), "Seismic response of underwater concrete pipes conveying fluid covered with nano-fiber reinforced polymer layer", *Soil Dynam. Earthq. Eng.*, **110**, 18-27. https://doi.org/10.1016/j.soildyn.2018.04.002

Hajmohammad, M.H., Nouri, A.H., Zarei, M.S. and Kolahchi, R. (2019a), "A new numerical approach and visco-refined zigzag theory for blast analysis of auxetic honeycomb plates integrated by multiphase nanocomposite facesheets in hygrothermal", *Eng. Comput*., **35**(4), 1141-1157. https://doi.org/10.1007/s00366-018-0655-x.

Hajmohammad, M.H., Kolahchi, R., Zarei, M.S. and Nouri, A.H. (2019b), "Dynamic response of auxetic honeycomb plates integrated with agglomerated CNT-reinforced face sheets subjected to blast load based on visco-sinusoidal theory", *Int. J. Mech. Sci*., **153**, 391-401. https://doi.org/10.1016/j.ijmecsci.2019.02.008.

Hajmohammad, M.H., Zarei, M.S., Kolahchi, R. and Karami, H. (2019c), "Visco-piezoelasticity-zigzag theories for blast response of porous beams covered by graphene platelet-reinforced piezo-electric layers", *J. Sandw. Struct. Mater*., 1099636219839175. https://doi.org/10.1177/1099636219839175.

Hajmohammad, M.H., Farrokhian, A. and Kolahchi, R. (2021), "Dynamic analysis in beam element of wave-piercing Catamarans undergoing slamming load based on mathematical modelling", *Ocean Eng*., **234**, 109269. https://doi.org/10.1016/j.oceaneng.2021.109269.

Jafarian Arani, A., and Kolahchi, R. (2016), "Buckling analysis of embedded concrete beams armed with carbon nanotubes", *Comput. Concr*., **17**(5), 567-578. https://doi.org/10.12989/cac.2016.17.5.567.

Keshtegar, B., Motezaker, M., Kolahchi, R. and Trung, N.T.

(2020a), "Wave propagation and vibration responses in porous smart nanocomposite sandwich beam resting on Kerr foundation considering structural damping", *Thin Wall. Struct.*, **154**, 106820. https://doi.org/10.1016/j.tws.2020.106820

Keshtegar, B., Farrokhian, A., Kolahchi, R. and Trung, N.T. (2020b), "Dynamic stability response of truncated nanocomposite conical shell with magnetostrictive face sheets utilizing higher order theory of sandwich panels", *Eur. J. Mech. A Solids*, **82**, 104010. https://doi.org/10.1016/j.euromechsol.2020.104010

Keshtegar, B., Tabatabaei, J., Kolahchi, R. and Trung, N.T. (2020c), "Dynamic stress response in the nanocomposite concrete pipes with internal fluid under the ground motion load", *Adv. Concr. Constr.*, **9**(3), 327-335. https://doi.org/10.12989/acc.2020.9.3.327.

Kolahchi, R., Rabani Bidgoli, M., Beygipoor, G. and Fakhar, M.H. (2013), "A nonlocal nonlinear analysis for buckling in embedded FG-SWCNT-reinforced microplates subjected to magnetic field", *J. Mech. Sci. Tech.*, **5**, 2342-2355. https://doi.org/10.1007/s12206-015-0811-9.

Kolahchi, R., Moniri Bidgoli, A.M. and Heydari, M.M. (2015), "Size-dependent bending analysis of FGM nano-sinusoidal plates resting on orthotropic elastic medium", *Struct. Eng. Mech.*, **55**(5), 1001-1014, http://doi.org/10.12989/sem.2015.55.5.1001.

Kolahchi, R., Safari, M. and Esmailpour, M. (2016a). "Dynamic stability analysis of temperature-dependent functionally graded CNT-reinforced visco-plates resting on orthotropic elastomeric medium", *Compos. Struct.*, 150, 255-265. https://doi.org/10.1016/j.compstruct.2016.05.023.

Kolahchi, R., Hosseini, H. and Esmailpour, M. (2016b). "Differential cubature and quadrature-Bolotin methods for dynamic stability of embedded piezoelectric nanoplates based on visco-nonlocal-piezoelasticity theories", *Compos. Struct.*, **157**, 174-186, https://doi.org/10.1016/j.compstruct.2016.08.032.

Kolahchi, R. and Moniribidgoli, A.M. (2016). "Size-dependent sinusoidal beam model for dynamic instability of single-walled carbon nanotubes", *Appl. Math. Mech.*, **37**(2), 265-274. https://doi.org/10.1007/s10483-016-2030-8.

Kolahchi, R. (2017), "A comparative study on the bending, vibration and buckling of viscoelastic sandwich nano-plates based on different nonlocal theories using DC, HDQ and DQ methods", *Aerosp. Sci. Tech.*, **66**, 235-248. https://doi.org/10.1016/j.ast.2017.03.016.

Kolahchi, R., Hosseini, H., Fakhar, M.H., Taherifar, R. and Mahmoudi, M. (2019), "A numerical method for magneto-hygro-thermal postbuckling analysis of defective quadrilateral graphene sheets using higher order nonlocal strain gradient theory with different movable boundary conditions", *Comput. Math. Appl.*, **78**, 2018-2034. https://doi.org/10.1016/j.camwa.2019.03.042.

Laureano, R.W., Mantari, J.L., Yarasca, J., Oktem, A.S., Monge, J. and Zhou, X. (2024a), "Exact solutions for clamped spherical and cylindrical panels via a unified formulation and boundary discontinuous method", *Compos. Struct.*, **346**, 118429. https://doi.org/10.1016/j.compstruct.2024.118429.

Laureano, R.W., Mantari, J.L., Yarasca, J., Oktem, A.S., Monge, J. and Zhou, X. (2024b), "A unified formulation and the boundary discontinuous Fourier method for clamped functionally graded shells", *Eng. Anal. Bound. Elem.*, **162**, 310-326. https://doi.org/10.1016/j.enganabound.2024.02.004.

Li, X., Liu, Y., Ge, L. and Zhang, Z. (2024), "A large-stroke reluctance-actuated nanopositioner: Compliant compensator for enhanced linearity and precision motion control", *IEEE ASME T. Mechatron.*, **29**(4), 2947-2955. https://doi.org/10.1109/TMECH.2024.3405195

Li, J., Wang, Z., Zhang, S., Lin, Y., Wang, L., Sun, C. and Tan, J. (2023), "A novelty mandrel supported thin-wall tube bending cross-section quality analysis: a diameter-adjustable multi-point contact mandrel", *J. Adv. Manuf. Technol.*, **124**(11), 4615-4637. https://doi.org/10.1007/s00170-023-10838-y

Lei, Z,. and Zhang, Y., (2018), "Characterizing buckling behavior of matrix-cracked hybrid plates containing CNTR-FG layers", *Steel Compos. Struct.*, **28**(4), 495-508. https://doi.org/10.12989/scs.2018.28.4.495

Mantari, J.L., Oktem, A.S. and Guedes Soares, C. (2011), "Static and dynamic analysis of laminated composite and sandwich plates and shells by using a new higher-order shear deformation theory", *Compos. Struct.*, **94**, 37-49. https://doi.org/10.1016/j.compstruct.2011.07.020.

Mantari, J.L., Oktem, A.S. and Guedes Soares, C. (2012), "A new higher order shear deformation theory for sandwich and composite laminated plates", *Compos. Part B Eng.*, **43**, 1489-1499. https://doi.org/10.1016/j.compositesb.2011.07.017.

Mantari, J.L. and Granados, E.V. (2014), "Optimized sinusoidal higher order shear deformation theory for the analysis of functionally graded plates and shells", *Compos. Part B Eng.*, **56**, 126-136, https://doi.org/10.1016/j.compositesb.2013.07.027.

Mantari, J.L. and Granados, E.V. (2015), "Dynamic analysis of functionally graded plates using a novel FSDT", *Compos. Part B Eng.*, **15**, 148-155. https://doi.org/10.1016/j.compositesb.2015.01.028.

Mantari, JL., Ramos, IA. and Zenkour, AM. (2016), "A unified formulation for laminated composite and sandwich plates subject to thermal load using various plate theories", *Int. J. Appl. Mech.*, **8**. https://doi.org/10.1142/S1758825116500873

Merzouki, T., Houari, M.S.A. and Tornabene, F. (2021), "Bending analysis of functionally graded porous nanocomposite beams based on a non-local strain gradient theory", *Math. Mech. Solids*, **27**. https://doi.org/10.1177/10812865211011759.

Motezaker, M. and Kolahchi, R. (2017a), "Seismic response of concrete columns with nanofiber reinforced polymer layer", *Comput. Concr.*, **20**(3), 361-368. https://doi.org/10.12989/cac.2017.20.3.361

Motezaker, M. and Kolahchi, R. (2017b), "Seismic response of SiO_2 nanoparticles-reinforced concrete pipes based on DQ and newmark methods", *Comput. Concr.*, **19**(6), 745-753. https://doi.org/10.12989/cac.2017.19.6.745

Motezaker, M., Kolahchi, R., Rajak, D.K. and Mahmoud, S.R. (2021a), "Influences of fiber reinforced polymer layer on the dynamic deflection of concrete pipes containing nanoparticle subjected to earthquake load", *Polym. Compos.*, **42**(8), 4073-4081. https://doi.org/10.1002/pc.26118

Motezaker, M., Jamali, M. and Kolahchi, R. (2021b), "Application of differential cubature method for nonlocal vibration, buckling and bending response of annular nanoplates integrated by piezoelectric layers based on surface-higher order nonlocal-piezoelasticity theory", *Comput. Appl. Math.*, **369**, 112625. https://doi.org/10.1016/j.cam.2019.112625

Pham, Q.H. Hoang, N.T., Tran, T.T. and and Zenkour, A. M. (2024), "Random vibration analysis of functionally graded sandwich plates with different skin layers subjected to double explosive load: Mathematical model with numerical solution proposition", *Arch. Civil Mech. Eng.*, **24**, 220. https://doi.org/10.1007/s43452-024-01027-z.

Polit, O. and Touratier, M. (2002), "A multilayered/sandwich triangular finite element applied to linear and non-linear analyses", *Compos. Struct.*, **58**, 121-128, https://doi.org/10.1016/S0263-8223(02)00033-8.

Ramos, I.A., Mantari, J.L. and Zenkour, A.M. (2016), "Laminated composite plates subject to thermal load using trigonometrical theory based on Carrera Unified Formulation", *Compos. Struct.*, **143**, 324-335. https://doi.org/10.1016/j.compstruct.2016.02.020.

Shahrany, H.D. and and Zenkour, A.M. (2024), "Control of dynamic response of the functionally graded smart sandwich

beam coupled variable Kelvin–Voigt–Pasternak's model", *Ain Shams Eng. J.*, **15**, 102476. https://doi.org/10.1016/j.asej.2023.102476.

Sobhani Aragh, B. (2017), "Mathematical modelling of the stability of carbon nanotube-reinforced panels", *Steel Compos. Struct.*, **24**, 727-740. https://doi.org/10.12989/scs.2017.24.6.727

Sun, L., Liang, T., Zhang, C. and Chen, J. (2023), "The rheological performance of shear-thickening fluids based on carbon fiber and silica nanocomposite", *Phys. Fl.*, **35**(3), 32002. https://doi.org/10.1063/5.0138294

Sun, L., Wang, G. and Zhang, C. (2024), "Experimental investigation of a novel high performance multi-walled carbon nano-polyvinylpyrrolidone/silicon-based shear thickening fluid damper", *J. Intell. Mater. Syst. Struct.*, **35**(6), 661-672. https://doi.org/10.1177/1045389X231222999

Taherifar, R., Zareei, S.A., Rabani Bidgoli, M. and Kolahchi, R. (2020), "Seismic analysis in pad concrete foundation reinforced by nanoparticles covered by smart layer utilizing plate higher order theory", *Steel Compos. Struct.*, **37**(1), 99-115, http://doi.org/10.12989/scs.2020.37.1.099.

Taherifar, R., Zareei, S.A., Rabani Bidgoli, M. and Kolahchi, R. (2021), "Application of differential quadrature and Newmark methods for dynamic response in pad concrete foundation covered by piezoelectric layer", *J. Comput. Appl. Math.*, **382**, 113075. https://doi.org/10.1016/j.cam.2020.113075.

Van Vinh, P. (2022), "Nonlocal free vibration characteristics of power-law and sigmoid functionally graded nanoplates considering variable nonlocal parameter", *Physica E*, **135**, 114951. https://doi.org/10.1016/j.physe.2021.114951

Wang, C., Wang, Z., Zhang, S., Liu, X. and Tan, J. (2023), "Reinforced quantum-behaved particle swarm-optimized neural network for cross-sectional distortion prediction of novel variable-diameter-die-formed metal bent tubes", *J. Comput. Des. Eng.*, **10**(3), 1060-1079. https://doi.org/10.1093/jcde/qwad037

Yarasca, J., Mantari, J.L., Monge, J.C. and Hinostroza, M.A. (2024), "A robust five-unknowns higher-order deformation theory optimized via machine learning for functionally graded plates", *Mech. Adv. Mater. Struct.*, 1-16. https://doi.org/10.1080/15376494.2024.2344037.

Yayli, M.Ö. (2017), "Buckling analysis of a cantilever single-walled carbon nanotube embedded in an elastic medium with an attached spring", *Micro Nano Lett.*, **12**, 255-259. https://doi.org/10.1049/mnl.2016.0662

Yang, Y,. Hu, Zh.L and FangLi, X.(2021), "Axisymmetric bending and vibration of circular nanoplates with surface stresses", *Thin Wall. Struct*, **166**, 108086. https://doi.org/10.1016/j.tws.2021.108086

Zamanian, M., Kolahchi, R. and Rabani Bidgoli, M. (2017), "Agglomeration effects on the buckling behaviour of embedded concrete beams reinforced with SiO2 nano-particles", *Wind Struct.*, **24**, 43-57. http://doi.org/10.12989/was.2017.24.1.043.

CC